ISSN 1392-1320 MATERIALS SCIENCE (MEDŽIAGOTYRA). Vol. 30, No. 3. 2024

The Nucleated Poly(L-lactic acid): The Role of a Phenylacetic Hydrazide Derivative

Ninghui TAN, Yang LV, Hao HUANG, Lisha ZHAO, Yanhua CAI *

Chongqing Key Laboratory of Environmental Materials & Remediation Technologies, College of Chemistry and Environmental Engineering, College of Pharmaceutical Sciences, Chongqing University of Arts and Sciences, Chongqing-402160, P.R. China

http://doi.org/10.5755/j02.ms.36050

Received 11 January 2024; accepted 28 February 2024

The melt-crystallization, cold-crystallization, melting behaviors, thermal stability, and optical properties of poly(L-lactic acid) (PLLA) nucleated by a phenylacetic hydrazide derivative (DAPH) were investigated. The melt-crystallization confirmed DAPH's heterogeneous nucleation role in improving PLLA's poor crystallization capability, concurrently DAPH loading, cooling rate and final melting temperature were three key factors affecting PLLA's melt-crystallization behaviors. The results from cold-crystallization indicated that the addition of DAPH could accelerate PLLA's cold-crystallization *via* cold-crystallization peak's shift toward the lower temperature side as DAPH loading increased. Through analysis of PLLA/DAPH's multiple melting behaviors after melt-crystallization, it was found that DAPH loading, the previous melt-crystallization and heating rate determined PLLA/DAPH's melting processes after melt-crystallization; and PLLA/DAPH's melting processes after isothermal crystallization depended on the previous crystallization temperature. A drop in thermal decomposition temperature for 5 wt.% mass loss suggested that pure PLLA has better thermal stability compared with PLLA/DAPH. Additionally, the introduction of DAPH could not improve PLLA's transparency, in contrast, the haze of PLLA was increased greatly owing to the existence of DAPH.

Keywords: poly(L-lactic acid), biodegradability, phenylacetic hydrazide, crystallization, transparency.

1. INTRODUCTION

In terms of solid waste, reducing the large-scale usage of petroleum-based plastics is an important measure for economic and environmentally sustainable development. To achieve the aforementioned goal, major attention has been shifted to biopolymers as alternatives to petroleum-based plastics. Poly(L-lactic acid) (PLLA) is a semi-crystalline polyester derived from renewable resources like corn, potato, starch and sugarcane [1, 2], and the advantages of PLLA, including biodegradability [3], compatibility [4], transparency [5], good processability [6] and non-toxic for the human body and the environment [7], has obtained increasing attention in the fields of disposable products [8], biomedicine [9 – 11], electronic device [12 – 14], automobile industry [15 – 17], For instance, PLLA was used as a base polymer to load and deliver the topical antibiotic, neomycin. The in vitro dissolution firstly exhibited first-order release kinetics for neomycin, followed by diffusion-controlled release after releasing for 20 h, and the ability to load neomycin onto PLLA increases threefold with molecular weight of polyethylene glycols coating decreasing from 20 kDa to 400 Da. This study exhibited potential applications in dermal regeneration and tissue engineering [18].

However, due to the limitation of some shortcomings like slow crystallization rate, poor heat resistance, brittleness, and high costs [19 – 21], numerous potential applications of PLLA are greatly reduced. Thus, up to now, a large number of studies need to be still performed to improve PLLA's performance by adding functional additives or blending with other polymers. Among these defects, the slow crystallization rate affects not only crystallinity of PLLA's product but also thermal and the mechanical properties [22], that is, obtaining PLLA materials with high crystallinity in a short timescale process such as injection moulding is a great challenge. For solving the slow crystallization rate, adding a nucleating agent is thought to be one of the most effective ways to accelerate PLLA's crystallization rate [22], because the role of a nucleating agent is to decrease nucleation surface free energy barrier *via* providing abundant heterogeneous nuclei in polymer matrix to induce crystallization in higher temperature region and at a faster cooling rate. Additionally, the nucleating agent exhibits some advantages such as simpler operation and usage, low dosage and significant nucleation ability [23, 24]. Ma et al [25] investigated the influence of different types of nucleating agents on PLLA's crystallization, in which 0.5 wt.% talc could shorten half-time of crystallization of PLLA from 8 min to 1.2 min during isothermal crystallization at 120 ºC, and 0.5 min for *N, N*-dibenzoyladipohydrazide, as well as 0.6 min for *N, N*-(ethane-1, 2-diyl)bis(*N*-phenyloxalamide). Li *et al* [26] reported that a furan-phosphamide derivative POCFA was used to be a nucleating agent for PLLA's crystallization, and the half-time of crystallization reduced by 80.2 % compared to pure PLLA, shortened from 6.41 min to 1.27 min after adding 5 wt.% POCFA, moreover, the introduction of

* Corresponding author. Tel.: +86-23-61162815; fax: +86-23-61162725.
E-mail: *caiyh651@aliyun.com* (Y.H Cai)

POCFA improved PLLA's tensile strength and flame retardant.

According to structural analysis of the reported nucleating agents for PLLA's crystallization, nucleating agents can be commonly classed into three categories [27], they are inorganic nucleating agents, organic small molecule nucleating agents and macromolecular nucleating agents. Organic small molecule nucleating agents, in comparison to inorganic nucleating agents or organic macromolecular nucleating agents, possess a remarkable advantage of flexible molecular structure construction, and some common structures like amide, benzene and alkyl chain are concluded as basic structures for promoting PLLA's crystallization. Thus many new organic compounds were synthesized to serve as a nucleating agent, or some existing commercial organic small molecule compounds were selected to evaluate their possibility as a nucleating agent for PLLA, these typical organic small molecule nucleating agents include benzoylhydrazine derivatives [28, 29], oxalamide derivatives [30, 31], 1H-benzotriazole derivatives [32, 33], urea compounds [34, 35], D-sorbitol [8], etc.

Even so, developing more efficient organic small molecule nucleating agent is still expected to meet increasing industrial requirements. To achieve the aforementioned purpose, more organic small molecule compounds with different structures need to be developed to evaluate their nucleation ability during PLLA's crystallization. In this work, a phenylacetic hydrazide derivative with decyl (DAPH), derived from phenylacetic hydrazide and dodecanedioic acid, was synthesized to serve as an organic small molecule nucleating agent for PLLA's crystallization. The detailed crystallization processes, melting behaviors, thermal decomposition and optical properties of PLLA modified by DAPH were investigated by differential scanning calorimeter (DSC), thermal gravimetric analyzer (TGA) and transmittance meter. This work may be beneficial for further understanding the structure activity relationship of molecular structure with nucleation effect, and providing a reference for developing efficient commercial nucleating agents for PLLA.

2. EXPERIMENTAL

2.1. Reagents and materials

To synthesize DAPH, two main chemical reagents phenylacetic hydrazide and dodecanedioic acid were purchased from Shanghai Titan Scientific Co., Ltd. Other chemical reagents, including *N*, *N*-Dimethylformamide (DMF), thionyl chloride, and pyridine, were obtained from Chongqing Huanwei Chemical Company. All chemical reagents were directly used without further purification. PLLA in this work was produced by Nature-Works LLC, and the trade name was 4032D.

2.2. Synthesis of DAPH and preparation of PLLA/DAPH

DAPH was synthesized in our lab, and the typical synthetic route includes two reaction steps as shown in Fig. 1, they are the acylation reaction of dodecanedioic acid and the amination reaction of phenylacetic hydrazide with dodecanedioyl dichloride. The detailed synthetic operation was similar to our previous works [36, 37], and the final khaki DAPH was dried over night at 45 °C under a vacuum to thoroughly remove residual water. Fourier Transform Infrared Spectrometer (FT-IR) υ: 3209.9, 3031.9, 2923.5, 2851.2, 1653.6, 1596.8, 1486.6, 1454.4, 1437.8, 1221.5, 1168.8, 939.4, 724.2, 695.5 cm^{-1}. ^1H Nuclear Magnetic Resonance (^1H NMR) δ: ppm; 10.01 (s, 1H, NH), 9.75 (s, 1H, NH), 7.22~7.33 (m, 5H, Ar), 3.36~3.45 (d, 2H, CH_2), 2.07~2.11 (t, 2H, CH_2), 1.48~1.49 (d, 2H, CH_2), 1.23 (s, 8H, CH_2). In addition, the geometry optimization of DAPH was carried out by Dmol3 calculation, and DAPH's optimized geometry structure and total electron density are displayed in Fig. 2.

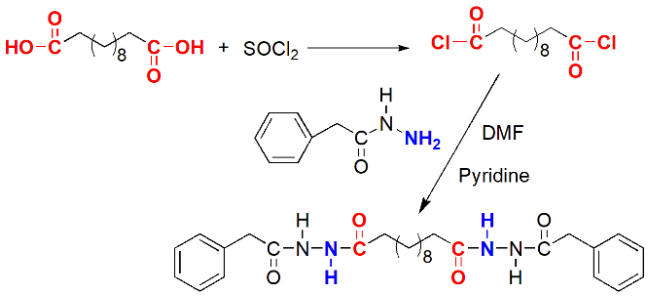

Fig. 1. Synthetic route of DAPH

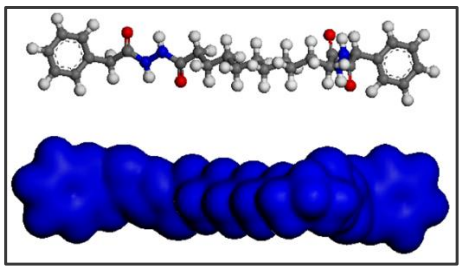

Fig. 2. Optimum geometry and total electron density of DAPH

The blend of PLLA and DAPH was performed in a counter-rotating mixer at 190 °C and a rotor speed of 32 rpm for 7 min and 64 rpm for 7 min, after that, the mixture containing various amounts of DAPH (0.4, 0.8, 1.5 and 3 wt.%) were obtained, and the corresponding modified PLLA were labeled as PLLA/0.4%DAPH, PLLA/0.8%DAPH, PLLA/1.5%DAPH and PLLA/3%DAPH, respectively. Then all the mixture were converted into sheets with 0.4 mm thickness by pressing at 10 MPa and 180 ºC for 5 min and then naturally cooled to room temperature.

2.3. Characterization and performance testing

Structure characterization. The molecular structure of DAPH was characterized by ^1H NMR (AVANCE 400MHz, Bruker, USA) and FT-IR (iS50, Thermo Fisher Scientific, USA). For ^1H NMR characterization, the spectra were referred to tetramethylsilane, and the deuterium reagent for dissolving DAPH was dimethyl sulfoxide. For FT-IR characterization, the traditional KBr pellet was used to prepare the DAPH testing sample, and the mixing mass ratio of KBr and DAPH was 150:1 before tableting, and the testing wavenumber was from 4000 cm^{-1} to 400 cm^{-1}.

Performance testing. All testing samples for DSC, TGA and optical properties were obtained by cutting the sheets

with 0.4 mm thickness. The crystallization and melting processes of pure PLLA and PLLA/DAPH were recorded by DSC (Q2000, TA instruments, USA) with 50 mL/min nitrogen. Although the detailed testing conditions are different, eliminating heat history and calibrating temperature and heat flow were carried out to ensure the same testing level. TGA (Q500, TA instruments, USA) was employed to record the effect of DAPH on PLLA's thermal stability in the air, and the testing temperature region was from room temperature to 650 °C at a heating rate of 5 °C/min. The light transmittance of pure PLLA and PLLA/DAPH were tested *via* a light transmittance meter (DR82, Donru Electronic Technology, China), and for a given sample, the average value of light transmittance was obtained through 5 times measurements.

3. RESULTS AND DISCUSSION

3.1. Melt-crystallization behavior

The goal of this study was to develop a new organic small molecule nucleating agent, therefore a comparative study on the melt-crystallization behavior of pure PLLA and PLLA/DAPH was first performed to evaluate DAPH's role. Fig. 3 is DSC thermograms of pure PLLA and PLLA/DAPH from the melt of 190 °C to 40 °C at a cooling rate of 1 °C/min. Compared to the DSC curve of pure PLLA, the DSC curve of any PLLA/DAPH exhibits an obvious and sharp melt-crystallization peak, there is no doubt that this difference depends on the effect of DAPH. For pure PLLA, on the one hand, poor nucleation ability prevents nuclei not being formed in the high temperature region, resulting in an extremely slow nucleation rate; on the other hand, the rigid structure of the PLLA molecular chain leads to its poor mobility in cooling, which seriously restricts PLLA crystal growth. Thus, pure PLLA can almost not form any crystal in cooling at 1 °C/min. In contrast, the existence of DAPH can provide abundant heterogeneous nuclei in the PLLA matrix, resulting in a very fast nucleation rate to promote nuclei to grow into crystals as soon as possible in the related high temperature region. As a result, an obvious and sharp melt-crystallization peak appears in DSC thermograms. In addition, Fig. 3 also displays the effect of DAPH loading on PLLA's melt-crystallization. It can be observed that PLLA/0.4%DAPH has the highest onset crystallization temperature (T_{oc}) of 136.7 °C and melt-crystallization peak temperature (T_{mc}) of 131.4 °C, as well as the largest melt-crystallization enthalpy (ΔH) of 50.9 J/g. However, PLLA/0.4%DABP exhibits a relatively wide melt-crystallization peak, meaning a relatively slow crystallization rate. Usually, the sharper the melt-crystallization peak is, the faster the crystallization rate is. With the increase of DAPH concentration from 0.4 wt.% to 1.5 wt.%, the width of the melt-crystallization peak visibly becomes narrow, indicating a faster crystallization rate. But when further increasing DAPH loading from 1.5 wt.% to 3 wt.%, the melt-crystallization peak exhibits an insignificant change in peak shape and position. In a word, the presence of DAPH as heterogeneous nuclei significantly accelerate PLLA's crystallization, and when DAPH concentration is less than 1.5 wt.%, PLLA/DAPH can achieve the fastest crystallization rate.

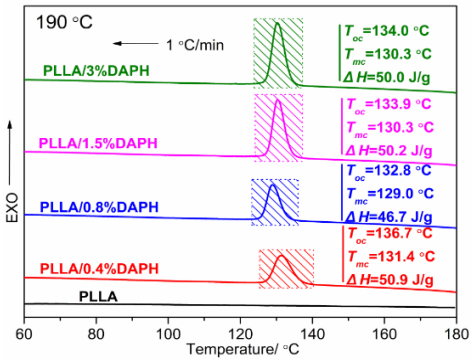

Fig. 3. Melt-crystallization DSC curves of pure PLLA and PLLA/DAPH from the melt of 190 °C to 40 °C at a cooling rate of 1 °C/min

A higher cooling rate is often expected to meet the requirements of industrial manufacturing, thus, the melt-crystallization behaviors at higher cooling rates were further studied by DSC. Fig. 4 shows DSC thermograms of PLLA/DAPH from the melt of 190 °C to 40 °C at different cooling rates.

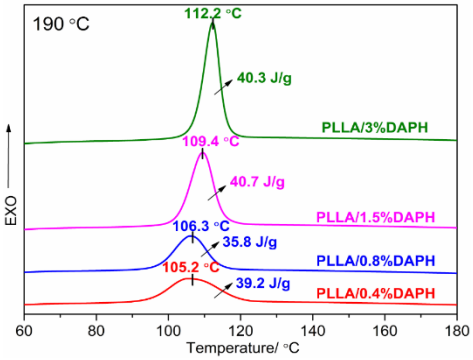

a

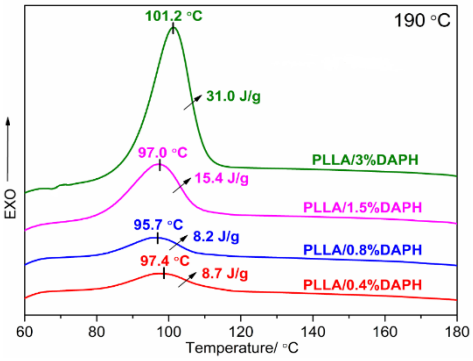

b

Fig. 4. DSC curves of PLLA/DAPH from the melt of 190 °C to 40 °C at different cooling rates: a – 10 °C/min; b – 20 °C/min

It is very clear that when increasing cooling rate from 10 °C/min to 20 °C/min, a given PLLA/DAPH evokes serious decrease in crystallization ability by analyzing phenomena that the melt-crystallization peak shifts toward the lower temperature side and becomes wider, suggesting that an increase of cooling rate leads to the delayed crystallization process [38], the reason is that the lagging response of PLLA segments motion to action frequency and rate of temperature variability. And this effect of cooling

rate on melt-crystallization can be easily found in other systems like PLA/cellulose fibres [39], PLA/talc [40], PLA/NT-20 [40], PLLA/BSAD [41], PLA/graphene [42], etc. It should be also noted that, when the cooling rate is the same, a larger amount of DAPH has an inhibition for decrease of crystallization ability, because PLLA containing a larger amount of DAPH exhibits a higher melt-crystallization peak temperature, and the effect of cooling rate on the melt-crystallization enthalpy is relatively small, even when the cooling rate is 20 °C/min, PLLA/3%DAPH has still the ΔH of 31.0 J/g. Although an increase in cooling rate weakens the crystallization ability of PLLA/DAPH, the melt-crystallization peaks of all PLLA/DAPH are still very obvious, confirming DAPH's powerful crystallization promoting ability for PLLA again.

In the melt-crystallization section, the final melting temperature (T_f) is another important influence factor for crystallization, because both DAPH's solubility in PLLA and the content of undissolved DAPH are dependent on T_f, and the undissolved DAPH and DAPH's solubility determine nuclei density and interaction of PLLA molecular chain with DAPH respectively, finally affecting PLLA's crystallization. The effects of T_f from 170 °C to 210 °C on melt-crystallization processes of PLLA/DAPH were presented in Fig. 5. As shown in Fig. 5, differing from other T_f, when the T_f is 170 °C, any a given PLLA/DAPH exhibits a very wide melt-crystallization peak, indicating a relatively slow crystallization rate and the fact that a low T_f is not conducive to the promotion of crystallization rate because of the decline of migration ability of PLLA molecular chain in low temperature region. According to crystallization process analysis, the appearance of a wide melt-crystallization peak is thought to be probably due to the slow crystal growth rate, because the existence of DAPH must possess a fast nucleation rate. What is worse, upon cooling from the T_f of 170 °C, PLLA containing a higher DAPH concentration exhibits a wider melt-crystallization peak, even the difference between T_{oc} and T_{mc} is up to 8.7 °C for PLLA/3%DAPH, the reason is that the mobility of PLLA molecular chain is inhibited by the excessive DAPH. However, the fact, that any PLLA/DAPH possesses the highest T_{oc} and T_{mc}, should not be ignored, meaning that the T_f of 170 °C can cause crystallization to occur in higher temperature regions. When further increasing T_f, overall the melt-crystallization peak firstly becomes narrow, and then becomes wide. When the T_f is 190 °C, apart from PLLA/0.4% DAPH, other PLLA/DAPH exhibit the sharpest melt-crystallization peak, showing the fastest crystallization rate.

3.2. Cold-crystallization behavior

The cold-crystallization heating processes of PLLA/DAPH were recorded to explore the effect of DAPH and its loading on PLLA's cold-crystallization behavior in depth. As described in the characterization and performance testing section, to ensure that the cold-crystallization test starts from the amorphous state, any PLLA/DAPH was quenched from the melt of 190 °C to 40 °C to reach the amorphous state, and then heated to 180 °C at the heating rate of 1 °C/min. As displayed in Fig. 6, DAPH loading is very important factor for affecting PLLA's cold-crystallization behavior.

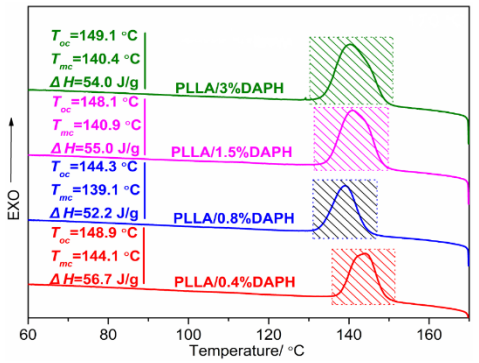

a

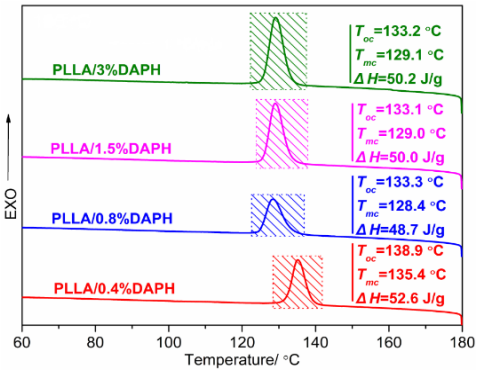

b

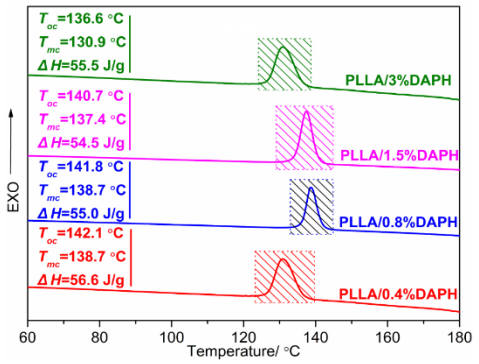

c

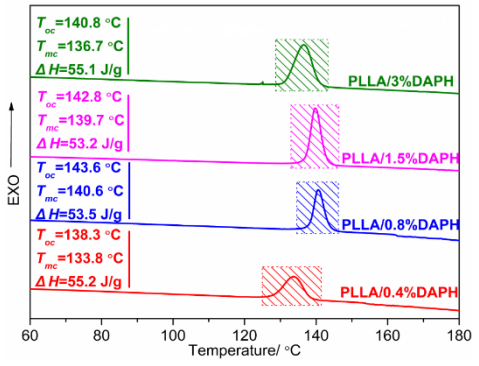

d

Fig. 5. DSC curves of PLLA/DAPH from different T_f at a cooling rate of 1 °C/min: a – 170 °C; b – 180 °C; c – 200 °C; d – 210 °C

In Fig. 6, the cold-crystallization peak temperatures of PLLA/0.4%DAPH, PLLA/0.8%DAPH, PLLA/1.5%DAPH and PLLA/3%DAPH are obtained, and the values for PLLA/0.4%DAPH, PLLA/0.8%DAPH, PLLA/1.5%DAPH and PLLA/3%DAPH are around 87.8 °C, 86.9 °C, 85.7 °C and 83.5 °C, respectively, shifting to lower temperature side as DAPH concentration increased, which implies that the DAPH can accelerate PLLA's cold crystallization, the similar results can also be found in PLLA/ovi-POSS [43], PLLA/NES [44] and PLLA/uracil [45].

Additionally, the difference in the resulting melting point of all PLLA/DAPH is almost negligible as shown in Fig. 6. However, the area of melting peak is relatively larger for PLLA/3%DAPH, as compared to PLLA containing a lower DAPH loading, overall this is because of the more crystals formed during the quenching and heating processes.

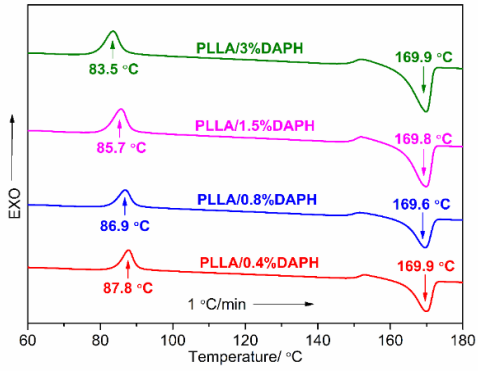

Fig. 6. DSC curves recorded in cold crystallization at a heating rate of 1 °C/min for PLLA/DAPH

3.3. Melting process

The heating curves of PLLA/DAPH after melt-crystallization at 1 °C/min are shown in Fig. 7. The influences of the heating rate on PLLA/DAPH's melting processes are visible, and either the single or double melting peaks can be observed. When the heating rate is higher than 5 °C/min, the double melting peaks cannot be observed, and the melting peak becomes wider as the heating rate further increases, this is mainly attributable to the influence of thermal inertia. Whereas PLLA/DAPH's melting behaviors exhibit very large difference when reducing the heating rate to below 5 °C/min; on one hand, the double melting peaks appear, and the double melting peaks mainly stem from PLLA containing a relative high DAPH loading; on the other hand, a drop in heating rate can accelerate PLLA with a relatively low DAPH loading to form double melting peaks, and for a given PLLA/DAPH, the slower the heating rate is, the more obvious the double melting peaks become, that is, the double melting peaks depend on the heating rate under this circumstance and high-temperature side melting peak with low-temperature side melting peak gradually merged into the single melting peak with increasing heating rate. Additionally, at a given heating rate, the appearance of high-temperature side melting peak is related to DAPH loading, in other words, the higher DAPH loading is, the more obvious PLLA/DAPH's high-temperature side melting peak exhibits. However, it is also the fact that PLLA/0.4%DAPH only exhibits a single melting peak at all heating rates, meaning that a low DAPH loading cannot make the previous defect-ridden crystalline lamellar recrystallize during heating.

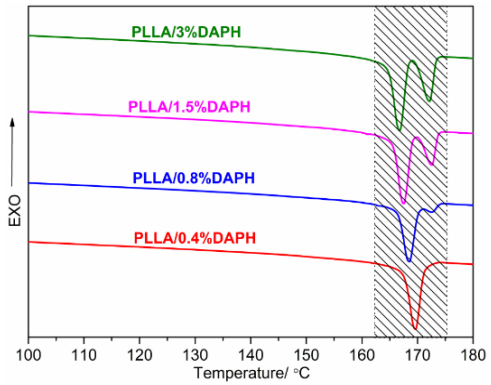

a

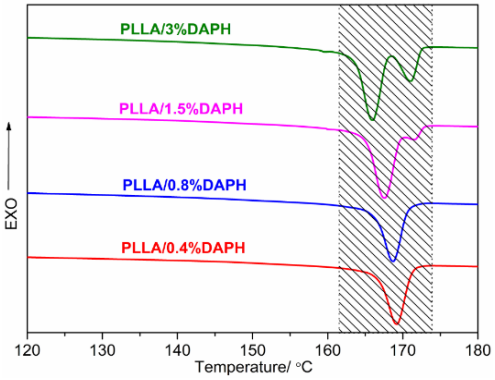

b

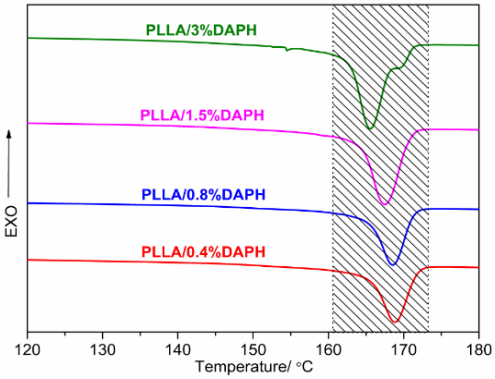

c

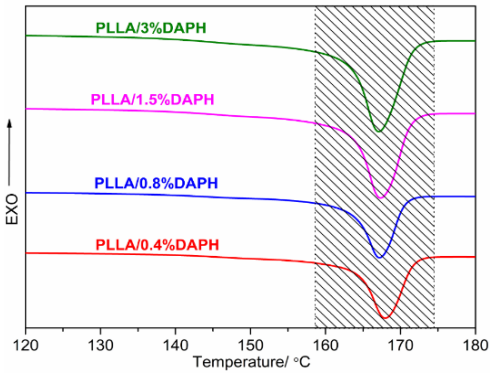

d

continued on next page

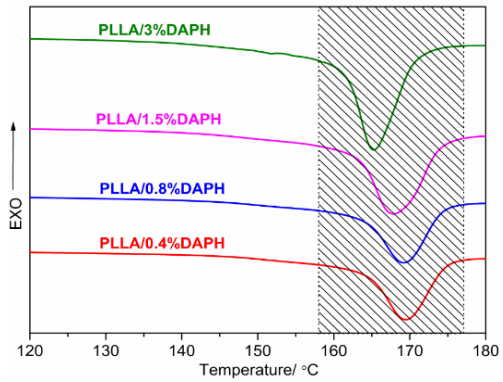

e

Fig. 7. DSC curves in melting processes at different heating rates after cooling at 1 ºC/min for PLLA/DAPH: a – 1 °C/min; b – 2 °C/min; c – 5 °C/min; d – 10 °C/min; e – 20 °C/min

Further, PLLA/DAPH's melting behaviors after going through different melt-crystallization *via* changing the rate were studied. Fig. 8 presents PLLA/DAPH's melting processes at different heating rates that corresponded to the rates of melt-crystallization at different cooling rates (1, 2, 3, 5 and 10 C/min). It is clear that an increase in rate causes high-temperature side melting peak appeares and becomes more and more obvious, the reason is that an increase in cooling rate cannot make PLLA macromolecular segments form a regular structure, leading to the appearance of small and imperfect crystals in melt-crystallization cooling stage, and these small and imperfect crystals can recrystallize during heating, as a result, the melt of these recrystallized crystals only occurred at a higher temperature.

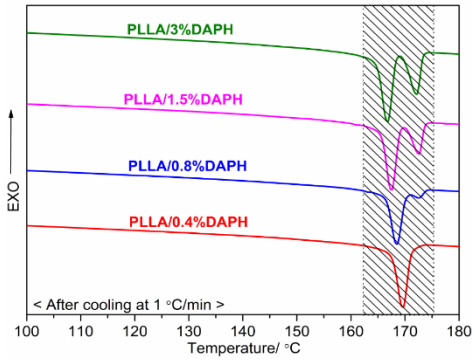

a

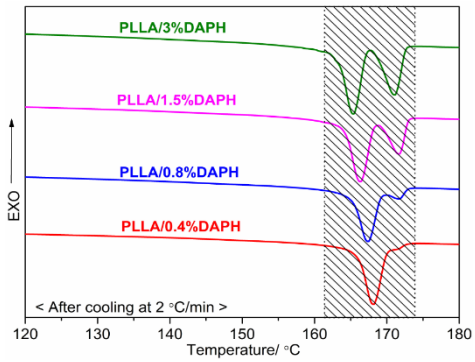

b

continued on next page

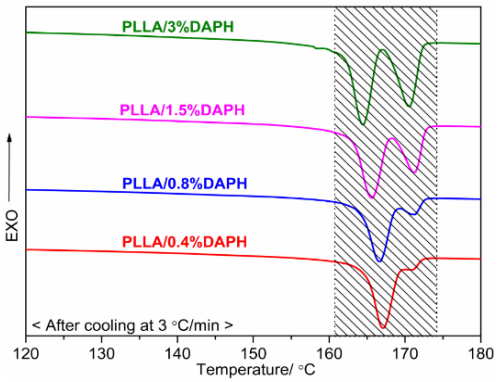

c

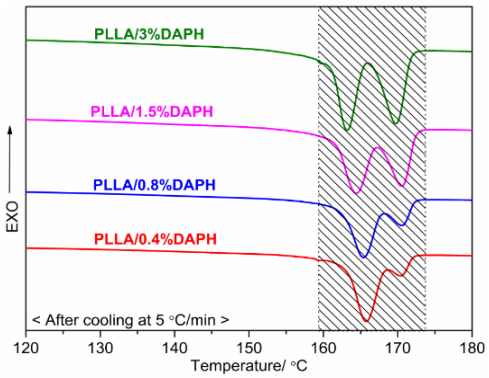

d

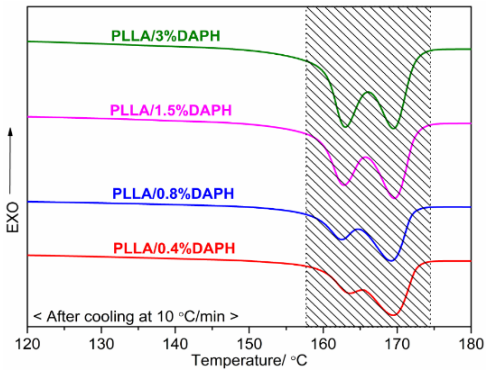

e

Fig. 8. DSC curves in melting processes at different heating rates corresponding to the rate of melt-crystallization at different cooling rates for PLLA/DAPH: a – 1 °C/min; b – 2 °C/min; c – 3 °C/min; d – 5 °C/min; e – 10 °C/min

In addition, the slow rate is conducive to crystal growth which can be evidenced by the sharper melting peaks, because the more perfect the crystals are, the sharper the melting peak is, and the shorter the melting range is. PLLA/DAPH's melting processes at a heating rate of 10 °C/min after isothermal crystallization were also recorded as seen in Fig.9. The crystallization time of 180 min can ensure sufficient crystallization. Fig. 9 focuses on the evaluation of the influence of crystallization temperature (T_c) on PLLA/DAPH's melting processes. With the reduction of T_c from 140 °C to 115 °C, the melting enthalpy of any PLLA/DAPH gradually decreases, suggesting that crystallinity significantly depends on T_c, because a higher melting enthalpy often represents higher crystallinity. Specifically, the decrease of the melting

enthalpy is from 60.3 J/g to 50.3 J/g for PLLA/3%DAPH, from 59.9 J/g to 49.1 J/g for PLLA/1.5%DAPH, from 57.4 J/g to 47.8 J/g for PLLA/0.8%DAPH and from 59.5 J/g to 50.1 J/g for PLLA/0.4%DAPH, respectively.

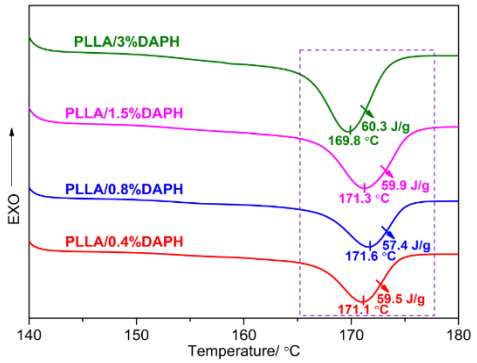

a

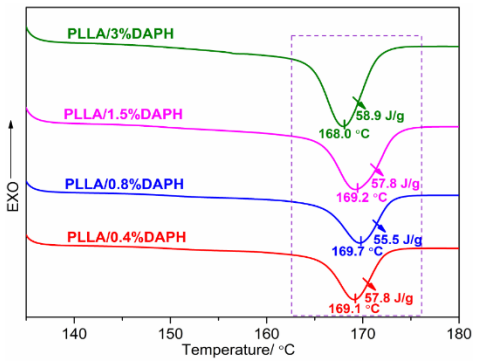

b

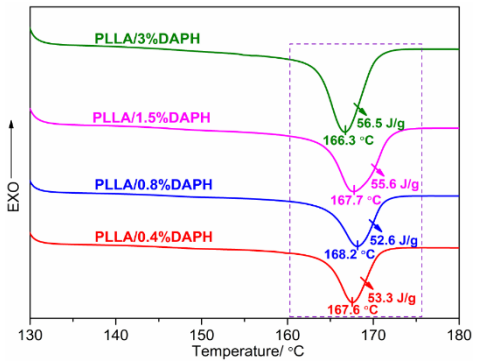

c

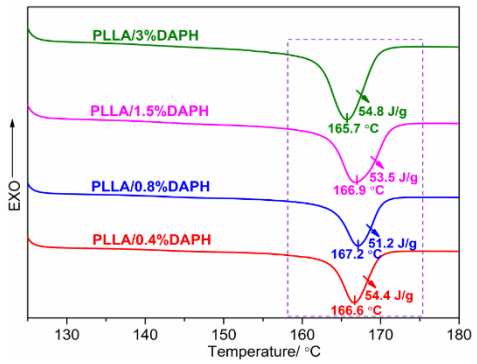

d

continued on next page

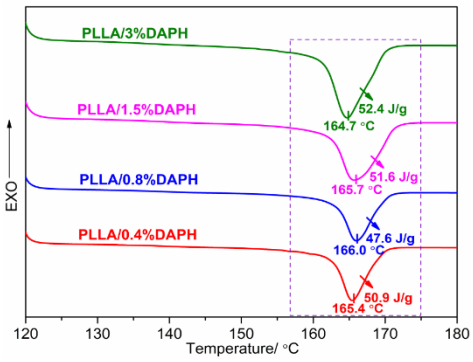

e

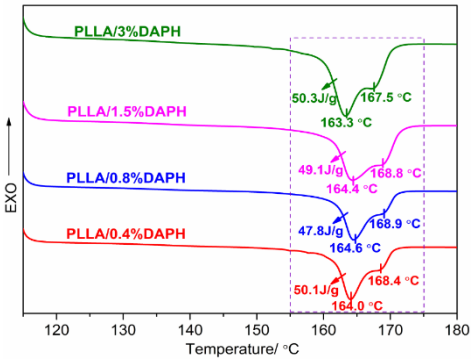

f

Fig. 9. Melting curves of PLLA/DAPH at a heating rate of 10 °C/min after isothermal crystallization at different T_c: a – 140 °C for 180 min; b – 135 °C for 180 min; c – 130 °C for 180 min; d – 125 °C for 180 min; e – 120 °C for 180 min; f – 115 °C for 180 min

Additionally, it can be seen from Fig. 9 that, when T_c is 115 °C, the double melting peaks appear indicating that there are regenerated crystals during heating. However, only the single melting peak appears, when T_c is higher than 115 °C, additionally, the melting peak of a given PLLA/DAPH shifts toward the lower-temperature side as T_c decreases, meaning that a higher T_c results in that the melt of crystals formed in isothermal crystallization stage occurs at the higher temperature. The reason may be that, when PLLA/DAPH was crystallized at a higher T_c, the formation of more crystals with more perfect crystallite structure becames easier, and the recrystallization during heating becames more difficult, finally resulting in the appearance of the single melting peak located at the higher temperature. In contrast, a low T_c restricts the mobility of the PLLA segment, leading to the appearance of smaller crystals with more defective crystallite structure, and it is easier for the recrystallization to occur during heating, as a result, the behavior for double melting peaks occurs. These results also indicate that double melting peaks in this study are attributed to melt-recrystallization mechanism [46].

3.4. Thermal stability and optical properties

DAPH's thermal stability determines the existential form of DAPH in the PLLA matrix and its effect on PLLA's thermal decomposition. Thus, it is necessary to investigate the thermal decomposition processes of DAPH, PLLA and PLLA/DAPH in air as shown in Fig. 10. Upon heating at 5 °C/min, the TGA curve of DAPH exhibits three main

thermal decomposition stages, and the thermal decomposition temperature for 5 wt.% mass loss ($T_{95\%}$) of DAPH is 213.6 °C, which is higher than the blending temperature of PLLA with DAPH, showing that ADPH as a single phase in PLLA matrix accelerate PLLA's crystallization after melting blend. Compared to the other two thermal mass loss stages, the first decomposition stage of DAPH has more than 50 % thermal mass loss. Whereas pure PLLA and four PLLA/DAPH samples exhibit one thermal decomposition stage, indicating that the addition of DAPH cannot almost change the thermal decomposition profile of PLLA, resulting from a relatively low DAPH loading in the PLLA matrix. Meantime, this thermal decomposition stage occurs in the temperature region from 270 °C to 370 °C, which originates from the chain scissions of ester groups and combustion [47]. Additionally, the $T_{95\%}$ of pure PLLA, PLLA/0.4%DAPH, PLLA/0.8%DAPH, PLLA/1.5%DAPH and PLLA/3%DAPH are obtained from Fig. 9, they are 320.8 °C for pure PLLA, 316.4 °C for PLLA/0.4%DAPH, 316.5 ºC for PLLA/0.8%DAPH, 310.9 °C for PLLA/1.5%DAPH and 300.4 °C for PLLA/3%DAPH, respectively. Through $T_{95\%}$ analysis, it is found that $T_{95\%}$ in general decreases with an increase in DAPH loading, two probable reasons are used to explain this result, one reason is the relatively low decomposition temperature of DAPH, and another reason is that PLLA containing a higher DAPH loading must possess more defects due to more or less incompatibility of PLLA with DAPH, and these defects are firstly destroyed in heating.

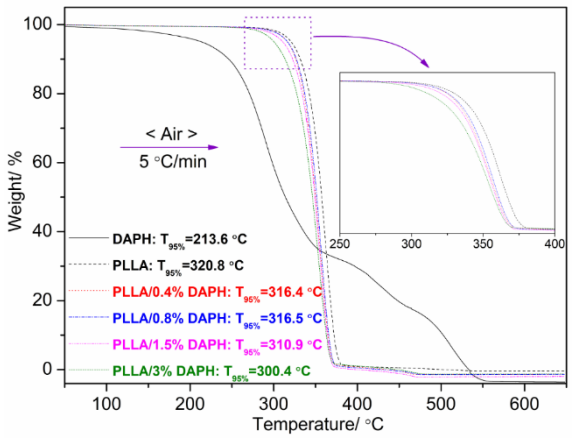

Fig. 10. TGA curves of DAPH, pure PLLA and PLLA/DAPH

Excellent transparency is one of the advantages of PLLA [5, 48], but blending with polymer or functional additives often affects PLLA's transparency. Fig. 11 displays PLLA and PLLA/DAPH's light transmittance, it is clear that the light transmittance continuously decreases as DAPH increases, even PLLA/3%DAPH is almost opaque. The main reason is proposed to be due to the effect of khaki DAPH; in addition, accelerating crystallization during processing may also decrease light transmittance because of an increase in crystallinity. Usually, crystallization can increase the refractive difference in a crystalline region with the amorphous region, and it is easy to refract and reflect at the interface, as a result, the light transmittance decreases. Upon the addition of 0.4 wt.% DAPH, there is a maximum drop of 26.0 % in light transmittance, but the drop gradually decreases from 26.0 % to 13.5 % with increasing DAPH concentration as seen in Fig. 11.

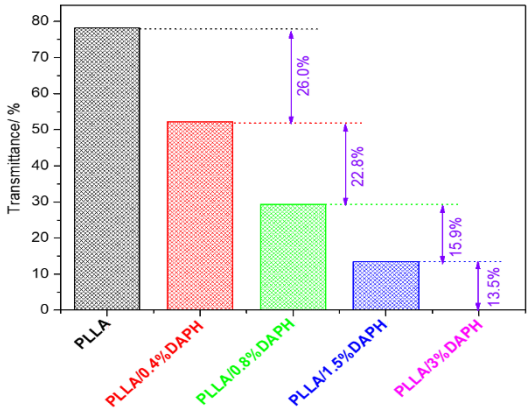

Fig. 11. Light transmittance of pure PLLA and PLLA/DAPH

4. CONCLUSIONS

In this study, DAPH could improve PLLA's poor crystallization ability by providing a heterogeneous nucleation site, overall DAPH loading and cooling rate exhibited the opposite effect on PLLA's melt-crystallization. Through comparative analysis of T_{oc} and T_{mc} during melt-crystallization, the T_f of 190 °C was thought to be conducive to promote PLLA's crystallization. Additionally, the addition of DAPH could accelerate PLLA's cold-crystallization, which be evidenced by the fact that the cold-crystallization peak shifted toward lower-temperature side and a cold-crystallization peak temperature decreased with increasing DAPH loading. PLLA/DAPH's melting processes after melt-crystallization greatly depended on the previous melt-crystallization, and a decrease in heating rate could cause double melting peaks to form; whereas PLLA/DAPH's melting behaviors after sufficient crystallization showed that T_c played a very important role in the following melting processes, because T_c significantly affected PLLA's isothermal crystallization behavior. The thermal decomposition curves of PLLA/DAPH exhibited one thermal decomposition stage as pure PLLA, but the existence of DAPH weakened PLLA's thermal stability due to the drop in $T_{95\%}$. An increase of PLLA/DAPH's haze, in comparison to pure PLLA, was thought to be resulting from DAPH's color itself and an increase of crystallinity.

Acknowledgments

This work was supported by Natural Science Foundation of Chongqing Science and Technology Bureau (project number CSTB2023NSCQ-MSX1087), Science and Technology Research Program of Chongqing Municipal Education Commission (project number KJZD-K202301303), and Chongqing University of Arts and Sciences (project number P2020HH06, and Y2023HH02).

REFERENCES

1. **Huang, A., Yu, P., Jing, X., Mi, H.Y., Geng, L.H., Chen, B.Y., Peng, X.F.** The Effect of Talc on the Mechanical, Crystallization and Foaming Properties of

Poly(Lactic Acid) *Journal of Macromolecular Science, Part B* 55 (9) 2016: pp. 908 – 924. https://doi.org/10.1080/00222348.2016.1217186

2. **Geng, Z.X., Zhen, W.J., Song, Z.B., Wang, X.F.** Structure and Performance of Poly(Lactic Acid)/Amide Ethylenediamine Tetraacetic Acid Disodium Salt Intercalation Layered Double Hydroxides Nanocomposites *Journal of Polymer Research* 25 (5) 2018: pp. 115-1 – 115-16. https://doi.org/10.1007/s10965-018-1482-x
3. **Yang, W.C., Wu, T., Chen, Y.L., Huang, Q.Y., Ao, J.Q., Ming, M., Gao, X.Y., Li, Z.Q., Chen, B.S.** Bionic Structure and Blood Compatibility of Highly Oriented Homo-epitaxially Crystallized Poly(L-Lactic Acid) *International Journal of Biological Macromolecules* 227 2023: pp. 749 – 761. https://doi.org/10.1016/j.ijbiomac.2022.12.192
4. **Banpean, A., Sakurai, S.** Confined Crystallization of Poly(Ethylene Glycol) in Spherulites of Poly (L-Lactic Acid) in a PLLA/PEG Blend *Polymer* 215 2021: pp. 123370-1 – 123370-15. https://doi.org/10.1016/j.polymer.2020.123370
5. **Olmo, J.A.D., Perez-Alvarez, L., Hernaez, E., Ruiz-Rubio, L., Vilas-Vilela, J.L.** Antibacterial Multilayer of Chitosan and (2-Carboxyethyl)-Beta-Cyclodextrin onto Polylactic Acid (PLLA) *Food Hydrocolloids* 88 2019: pp. 228 – 236. https://doi.org/10.1016/j.foodhyd.2018.10.014
6. **Faria, E.D., Dias, M.L., Ferreira, L.M., Tavares, M.I.B.** Crystallization Behavior of Zinc Oxide/Poly(Lactic Acid) Nanocomposites *Journal of Thermal Analysis and Calorimetry* 146 2021: pp. 1483 – 1490. https://doi.org/10.1007/s10973-020-10166-3
7. **Dzierzkowska, E., Scislowska-Czarnecka, A., Kudzin, M., Bogun, M., Szatkowski, P., Gajek, M., Kornaus, K., Chadzinska, M., Stodolak-Zych, E.** Effects of Process Parameters on Structure and Properties of Melt-blown Poly(lactic acid) Nonwovens for Skin Regeneration *Journal of Functional Biomaterials* 12 (1) 2021: pp. 16-1 – 16-17. https://doi.org/10.3390/jfb12010016
8. **Zhang, X., Yang, B., Fan, B.M., Sun, H., Zhang, H.J.** Enhanced Nonisothermal Crystallization and Heat Resistance of Poly(L-Lactic Acid) by D-Sorbitol as a Homogeneous Nucleating Agent *ACS Macro Letters* 10 (1) 2021: pp. 154 – 160. https://doi.org/10.1021/acsmacrolett.0c00830
9. **Salahuddin, N., Abdelwahab, M., Gaber, M., Elneanaey, S.** Synthesis and Design of Norfloxacin Drug Delivery System Based on PLA/TiO_2 Nanocomposites: Antibacterial and Antitumor Activities *Materials Science & Engineering C-Materials for Biological Applications* 108 2020: pp. 110337-1 – 110337-11. https://doi.org/10.1016/j.msec.2019.110337
10. **Ghamkhari, A., Abbaspour-Ravasjani, S., Talebi, M., Hamishehkar, H., Hamblin, M.R.** Development of a Graphene Oxide-Poly Lactide Nanocomposite as a Smart Drug Delivery System *International Journal of Biological Macromolecules* 169 2021: pp. 521 – 531. https://doi.org/10.1016/j.ijbiomac.2020.12.084
11. **Chi, H.Y., Chan, V.C., Li, C., Hsieh, J.H., Lin, P.H., Tsai, Y.H., Chen, Y.** Fabrication of Polylactic Acid/Paclitaxel Nano Fibers by Electrospinning for Cancer Therapeutics *BMC Chemistry* 14 (1) 2020: pp. 63-1 – 63-12. https://doi.org/10.21203/rs.3.rs-52756/v2
12. **Xue, B., Cheng, Z.L., Yang, S.D., Sun, X., Xie, L., Zheng, Q.** Extensional Flow-Induced Conductive Nanohybrid Shish in Poly(Lactic Acid) Nanocomposites toward Pioneering Combination of High Electrical Conductivity, Strength, and Ductility *Composites Part B-Engineering* 207 2021: pp. 108556-1 – 108556-9. https://doi.org/10.1016/j.compositesb.2020.108467
13. **Serrano, W., Melendez, A., Ramos, I., Pinto, N.J.** Poly(Lactic Acid)/Poly(3-Hexylthiophene) Composite Nanofiber Fabrication for Electronic Applications *Polymer International* 65 (5) 2016: pp. 503 – 507. https://doi.org/10.1002/pi.5081
14. **Mattana, G., Briand, D., Marette, A., Quintero, A.V., de Rooij, N.F.** Polylactic Acid as a Biodegradable Material for All-Solution-Processed Organic Electronic Devices *Organic Electronics* 17 2015: pp. 77 – 86. https://doi.org/10.1016/j.orgel.2014.11.010
15. **Yang, X., Fan, W., Ge, S.B., Gao, X.Z., Wang, S.J., Zhang, Y.H., Foong, S.Y., Liew, R.K., Lam, S.S., Xia, C.L.** Advanced Textile Technology for Fabrication of Ramie Fiber PLA Composites with Enhanced Mechanical Properties *Industrial Crops and Products* 162 2021: pp. 113312-1 – 113312-11. https://doi.org/10.1016/j.indcrop.2021.113312
16. **Notta-Cuvier, D., Odent, J., Delille, R., Murariu, M., Lauro, F., Raquez, J.M., Bennani, B., Dubois, P.** Tailoring Polylactide (PLA) Properties for Automotive Applications: Effect of Addition of Designed Additives on Main Mechanical Properties *Polymer Testing* 36 2014: pp. 1 – 9. https://doi.org/10.1016/j.polymertesting.2014.03.007
17. **Gokarneshan, N., Jeyanthi, B., Lakshmanaraj, S., Kumar, P.M.** Suitability of PLA Fibers as an Alternative to PET Fibers in Automotive Textiles *China Textile Science* 5 2010: pp. 39 – 41.
18. **Mahima, S., Sriramakamal, J.** Design and Characterization of 3D Printed, Neomycin-Eluting Poly-L-Lactide Mats for Wound-Healing Applications *Journal of Materials Science. Materials in Medicine* 32 (4) 2021: pp. 44-1 – 44-13. https://doi.org/10.1007/s10856-021-06509-7
19. **Haeldermans, T., Samyn, P., Cardinaels, R., Vandamme, D., Vanreppelen, K., Cuypers, A., Schreurs, S.** Poly(Lactic Acid) Bio-Composites Containing Biochar Particles: Effects of Fillers and Plasticizer on Crystallization and Thermal Properties *Express Polymer Letters* 15 (4) 2021: pp. 343 – 360. https://doi.org/10.3144/expresspolymlett.2021.30
20. **Barletta, M., Pizzi, E.** Optimizing Crystallinity of Engineered Poly(Lactic Acid)/Poly(Butylene Succinate) Blends: The Role of Single and Multiple Nucleating Agents *Journal of Applied Polymer Science* 138 (16) 2021: pp 50236. https://doi.org/10.1002/app.50236
21. **Kassos, N., Kelly, A.L., Gough, T., Gill, A.A.** Acceleration of Crystallisation Rate in Injection Moulded PLLA by Stereocomplex Formation *Materials Research Express* 7 (10) 2020: pp. 105308-1 – 105308-11. https://doi.org/10.1088/2053-1591/abbeba
22. **Khwanpipat, T., Seadan, M., Suttiruengwong, S.** Effect of PDLA and Amide Compounds as Mixed Nucleating Agents on Crystallization Behaviors of Poly(L-Lactic Acid) *Materials* 11 2018: pp. 1139-1 – 1139-10. https://doi.org/10.3390/ma11071139
23. **Xu, X.K., Zhen, W.J., Bian, S.Z.** Structure, Performance and Crystallization Behavior of Poly(Lactic Acid)/Humic

Acid Amide Composites *Polymer-Plastics Technology and Engineering* 57 (18) 2018: pp. 1858 – 1872. https://doi.org/10.1080/03602559.2018.1434670

24. **Zhao, L.S., Cai, Y.H.** Thermal Performances and Fluidity of Biodegradable Poly(L-Lactic Acid) Filled with *N, N'*-oxalyl Bis(Piperonylic Acid) Dihydrazide as a Nucleating Agent *Materials Science (Medžiagotyra)* 27 (4) 2021: pp. 458 – 465. https://doi.org/10.5755/j02.ms.25139
25. **Feng, Y.Q., Ma, P.M., Xu, P.W., Wang, R.Y., Dong, W.F., Chen, M.Q., Joziasse, C.** The Crystallization Behavior of Poly(lactic acid) with Different Types of Nucleating Agents *International Journal of Biological Macromolecules* 106 2018: pp. 955 – 962. https://doi.org/10.1016/j.ijbiomac.2017.08.095
26. **Sun, J.H., Li, L., Li, J.** Effects of Furan-Phosphamide Derivative on Flame Retardancy and Crystallization Behaviors of Poly(Lactic Acid) *Chemical Engineering Journal* 369 2019: pp. 150 – 160. https://doi.org/10.1016/j.cej.2019.03.036
27. **Jiang, L., Shen, T., Xu, P., Zhao, X., Li, X., Dong, W., Ma, P., Chen, M.** Crystallization Modification of Poly(Lactide) by Using Nucleating Agents and Stereocomplexation *E-Polymers* 16 2016: pp. 1 – 3. https://doi.org/10.1515/epoly-2015-0179
28. **Kawamoto, N., Sakai, A., Horikoshi, T., Urushihara, T., Tobita, E.** Nucleating Agent for Poly(L-Lactic Acid)-an Optimization of Chemical Structure of Hydrazide Compound for Advanced Nucleation Ability *Journal of Applied Polymer Science* 103 (1) 2007: pp. 198 – 203. https://doi.org/10.1002/app.25109
29. **Fan, Y.Q., Yan, S.F., Yin, J.B.** The Relationship Between Solubility and Nucleating Effect of Organic Nucleating Agent in Poly(L-Lactic Acid) *Journal of Applied Polymer Science* 136 (7) 2019: pp. 46851-1 – 46851-11. https://doi.org/10.1002/app.46851
30. **Shen, T.F., Xu, Y.S., Cai, X.X., Ma, P.M., Dong, W.F., Chen, M.Q.** Enhanced Crystallization Kinetics of Poly(lactide) with Oxalamide Compounds as Nucleators: Effect of Space Length Between the Oxalamide Moieties *RSC Advances* 6 (54) 2016: pp. 48365 – 48374. https://doi.org/10.1039/C6RA04050K
31. **Ma, P.M., Xu, Y.S., Wang, D.W., Dong, W.F., Chen, M.Q.** Rapid Crystallization of Poly(Lactic Acid) by Using Tailor-Made Oxalamide Derivatives as Novel Soluble-Type Nucleating Agents *Industrial & Engineering Chemistry Research* 53 (32) 2014: pp. 12888 – 12892. https://doi.org/10.1021/ie502211j
32. **Cai, Y.H., Tang, Y., Zhao, L.S.** Poly(L-Lactic Acid) with Organic Nucleating Agent *N, N, N'*-Tris(1H-Benzotriazole) Trimesinic Acid Acethydrazide: Crystallization and Melting Behavior *Journal of Applied Polymer Science* 132 (32) 2015: pp. 42402-1 – 42402-7. https://doi.org/10.1002/app.42402
33. **Cai, Y.H., Zhao, L.S., Zhang, Y.H.** Role of *N, N'*-Bis(1H-Benzotriazole) Adipic Acid Acethydrazide in Crystallization Nucleating Effect and Melting Behavior of Poly(L-Lactic Acid) *Journal of Polymer Research* 22 2015: pp. 246-1 – 246-9. https://doi.org/10.1007/s10965-015-0887-z
34. **Xu, Y.T., Wu, L.B.** Synthesis of Organic Bisurea Compounds and Their Roles as Crystallization Nucleating Agents of Poly(L-Lactic Acid) *European Polymer Journal* 49 2013: pp. 865 – 872. https://doi.org/10.1016/j.eurpolymj.2012.12.015
35. **Zheng, H.M., Ma, M., Zheng, Q.Q., Zhou, C.W., Chen, S., Wang, X.** Effect of Acylamino Nucleating Agent on Crystallization Behavior of Poly(L-Lactic Acid) *Journal of Materials Sciences & Engineering* 34 (6) 2016: pp. 941 – 946. (In Chinese) https://doi.org/10.14136/j.cnki.issn1673-2812.2016.06.016
36. **Zhao, L.S., Cai, Y.H.** Modified PLLA: Effect of BPADD on Properties *Green Materials* 8 (4) 2020: pp. 209 – 220. https://doi.org/10.1680/jgrma.20.00002
37. **Zhao, L.S., Qiao, J., Chen, W., Cai, Y.H.** Study on Thermal and Mechanical Properties of *N, N'*-Bis(Phenyl) 1, 4-Naphthalenedicarboxylic Acid Dihydrazide Nucleated Biodegradable Poly(L-Lactic Acid) *Polimery* 66 (4) 2021: pp. 234 – 244. https://doi.org/10.14314/polimery.2021.4.3
38. **Papageorgiou, G.Z., Achilias, D.S., Bikiaris, D.N.** Crystallization Kinetics of Biodegradable Poly(Butylene Succinate) Under Isothermal and Non-Isothermal Conditions *Macromolecular Chemistry and Physics* 208 (12) 2007: pp. 1250 – 1264. https://doi.org/10.1002/macp.200700084
39. **Behalek, L., Boruvka, M., Brdlik, P., Habr, J., Lenfeld, P., Kroisova, D., Veselka, F., Novak, J.** Thermal Properties and Non-Isothermal Crystallization Kinetics of Biocomposites Based on Poly(Lactic Acid), Rice Husks and Cellulose Fibers *Journal of Thermal Analysis and Calorimetry* 142 (2) 2020: pp. 629 – 649. https://doi.org/10.1007/s10973-020-09894-3
40. **Chen, L., Dou, Q.** Influence of the Combination of Nucleating Agent and Plasticizer on the Non-Isothermal Crystallization Kinetics and Activation Energies of Poly(Lactic Acid) *Journal of Thermal Analysis and Calorimetry* 139 2020: pp. 1069 – 1090. https://doi.org/10.1007/s10973-019-08507-y
41. **Fan, Y.Q., Yu, Z.Y., Cai, Y.H., Hu, D.D., Yan, S.F., Chen, X.S., Yin, J.B.** Crystallization Behavior and Crystallite Morphology Control of Poly(L-Lactic Acid) Through *N, N'*-Bis(Benzoyl) Sebacic Acid Dihydrazide *Polymer International* 62 (4) 2013: pp. 647 – 657. https://doi.org/10.1002/pi.4342
42. **Yang, B., Wang, D., Chen, F., Su, L.F., Miao, J.B., Chen, P., Qian, J.S., Xia, R., Liu, J.W.** Melting and Crystallization Behaviors of Poly(Lactic Acid) Modified with Graphene Acting as a Nucleating Agent *Journal of Macromolecular Science, Part B Physics* 58 (2) 2019: pp. 290 – 304. https://doi.org/10.1080/00222348.2018.1564222
43. **Yu, J., Qiu, Z.B.** Isothermal and Nonisothermal Cold Crystallization Behaviors of Biodegradable Poly(L-Lactide)/Octavinyl-Polyhedral Oligomeric Silsesquioxanes Nanocomposites *Industrial & Engineering Chemistry Research* 50 (22) 2011: pp. 12579 – 12586. https://doi.org/10.1021/ie201691y
44. **Li, Y., Han, C.Y., Yu, Y.C., Xiao, L.G., Shao, Y.** Isothermal and Nonisothermal Cold Crystallization Kinetics of Poly(L-Lactide)/Functionalized Eggshell Powder Composites *Journal of Thermal Analysis and Calorimetry* 131 (3) 2018: pp. 2213 – 2223. https://doi.org/10.1007/s10973-017-6783-5
45. **Pan, P.J., Yang, J.J., Shan, G.R., Bao, Y.Z., Weng, Z.X., Inoue, Y.S.** Nucleation Effects of Nucleobases on the Crystallization Kinetics of Poly(L-Lactide) *Macromolecular Materials and Engineering* 297 (7) 2012: pp. 670 – 679. https://doi.org/10.1002/mame.201100266

46. **He, Y., Fan, Z.Y., Hu, Y.F., Wu, T., Wei, J., Li, S.M.** DSC Analysis of Isothermal Melt-Crystallization, Glass Transition and Melting Behavior of Poly(L-Lactide) with Different Molecular Weights *European Polymer Journal* 43 (10) 2007: pp. 4431 – 4439. https://doi.org/10.1016/j.eurpolymj.2007.07.007

47. **Cai, Y.H., Zhao, L.S.** Investigating on the Modification of *N, N'*-Adipic Bis(Benzoic Acid) Dihydrazide on Poly(L-Lactic Acid) *Polymer Bulletin* 76 (5) 2019: pp. 2295 – 2310. https://doi.org/10.1007/s00289-018-2498-4

48. **Gallos, A., Crowet, J.M., Michely, L., Raghuwanshi, V.S., Mention, M.M., Langlois, V., Dauchez, M., Garnier, G., Allais, F.** Blending Ferulic Acid Derivatives and Polylactic Acid into Biobased and Transparent Elastomeric Materials with Shape Memory Properties *Biomacromolecules* 22 (4) 2021: pp. 1568 – 1578. https://doi.org/10.1021/acs.biomac.1c00002